Journal of Operation and Automation in Power Engineering

vol. 13, no. Special Issue, Dec. 2025, Pages: 101-113

http://joape.uma.ac.ir

Research Paper

Impact of Electric Vehicle Integration on Power Distribution Networks Considering Energy Pricing and Load Management Strategies

Bunyodjon Erdanayev [1, *], *Zokir Mamadiyarov* [2, 3], *Kamola Miraliyevna Yuldasheva* [4], *Akrom Normuxammadovich Erkaev* [5], *Nigora Turopova* [6], *Abdusalim Tukhtakuziyev* [7], and *Laylo Frunzeyevna Sharipova* [8]

[1]*Termez University of Economics and Service, Termez, Uzbekistan.*
[2]*Mamun University, Khiva, Uzbekistan.*
[3]*Alfraganus University, Tashkent, Uzbekistan.*
[4]*International School of Finance Technology and Science, Tashkent, Uzbekistan.*
[5]*Uzbekistan State World Languages University, 21A Building, 9A Block, Small Ring Road Street, Uchtepa District, Tashkent, Uzbekistan.*
[6]*Termez State University, 190100, Termez, Uzbekistan.*
[7]*Scientific-Research Institute of Agricultural Mechanization, Samarkand Str. 41, Yangiyul Dis., Tashkent Reg., Uzbekistan.*
[8]*Bukhara State Pedagogical Institute, Bukhara, Uzbekistan.*

Abstract— *This research initially examines the concepts related to distribution networks, electric vehicles (EVs), distributed generation sources, and EV load management programs over a 24-hour period from an energy pricing perspective. This analysis aims to optimize energy utilization and enhance system parameters. Additionally, the presence of renewable energy sources, such as solar energy, in the network is considered. For a distribution network incorporating distributed generation sources with variable energy prices, a load management program was implemented to optimize EV charging throughout the day. The proposed method was designed with the objectives of minimizing operational costs, power losses, and voltage drops while considering network loads in the presence of EVs. The total losses in a 33-bus network with the assumed hourly loads indicate that implementing demand response (DR) reduces network losses, whereas the presence of EVs increases these losses. Simulation results show that coordinated EV–DR scheduling effectively shifts charging away from peak hours, reduces daily operational cost by up to 7.4%, limits EV-induced loss increases from 19.4% to 6.1%, and improves voltage profiles while maintaining all network constraints. The results demonstrate that integrating EV flexibility with price-driven demand response provides a practical and effective solution for mitigating the adverse impacts of EV penetration and enhancing renewable energy utilization in distribution networks.*

Keywords—Electric vehicles, power distribution networks, distributed generation, demand response, power losses, voltage stability.

1. INTRODUCTION

In recent years, EVs have attracted increasing attention as viable alternatives to conventional internal combustion engine vehicles [1]. Their adoption is largely motivated by the potential to reduce dependence on fossil fuels and lower greenhouse gas emissions [2]. Nevertheless, large-scale EV deployment also introduces operational challenges for power systems, particularly when charging occurs in an uncoordinated manner, leading to increased peak demand and potential voltage and congestion problems [3]. Therefore, this study focuses on the optimal scheduling of EV charging and energy storage as an effective strategy to mitigate these impacts and improve overall network performance [4].

Sagaria *et al.* [5] introduced three types of EVs that are utilized for vehicle-to-grid (V2G) applications: battery electric vehicles (BEVs), fuel cell vehicles (FCVs), and hybrid electric vehicles (HEVs). BEVs store energy electrochemically in batteries [6]. Since these vehicles must be connected to the grid for charging, the additional costs associated with implementing V2G for them are negligible. Ma *et al.* [7] consider plug-in hybrid electric vehicles (PHEVs) as the next generation of EVs, combining the high efficiency of BEVs with the extended range of conventional vehicles. Current designs of these vehicles have an all-electric range of approximately 20 to 40 miles (equivalent to 32 to 64 km). In [8] calculated the V2G capacity required to stabilize solar power for peak demand and wind power for base load. According to their study, four V2G-related market applications

Received: 30 Nov. 2025
Revised: 27 Dec. 2025
Accepted: 29 Dec. 2025
*Corresponding author:
E-mail: bunyodjon_erdanayev@tues.uz (B. Erdanayev)
DOI: 10.22098/joape.2025.18934.2474

include base load support, peak shaving, spinning reserve, and frequency regulation. They argue that V2G is not suitable for base load applications but can be utilized for peak shaving under certain conditions. Additionally, it is competitive for spinning reserves and highly competitive for frequency regulation. In [9] stated that the development of the V2G concept has three positive effects on air pollution. First, by creating a source of income, it encourages vehicle owners to adopt electric vehicles. Second, since peak and emergency power generation primarily rely on fossil fuel-based power plants, which are often located near densely populated areas, V2G can help reduce the pollution generated by these sources. Third, V2G can mitigate the environmental impact of peak and emergency power generation. According to Singh *et al*. [10], the advantages of V2G include peak load reduction and, consequently, decreased congestion in the transmission network. Other benefits include reduced line losses, deferred investment in transmission infrastructure, and reduced operational pressure on the power system.

Additionally, electric vehicles can participate in ancillary service markets. Tariq *et al*. [11] conducted a study on optimal charging profiles to increase energy consumption during off-peak hours, while Hariri *et al*. [12] examined the impact of charging profiles on the distribution network. In general, most research on electric vehicles has focused on optimal charging scheduling to achieve desirable performance indicators, such as minimizing losses, improving voltage profiles, and utilizing V2G technology as an energy storage solution. The placement of V2G parking stations, considering power losses and reliability constraints as economic factors, was implemented by [13]. Furthermore, in [14] proposed a charging algorithm that facilitates load increase during off-peak hours. A common aspect of these studies is the focus on EV charging planning. However, given the uncertainties in EV owners' behavior, the potential lack of participation in these charging programs, and the battery degradation caused by frequent irregular charging and discharging, the economic and technical feasibility of such implementations remains a challenge.

With the increasing penetration of EVs into distribution systems, the total load imposed on medium- and low-voltage networks rises significantly. In practice, most EV owners tend to plug in their vehicles upon arrival at home, typically during the early evening [15]. If such charging is left uncoordinated, the resulting clustering of demand often coincides with existing residential peak loads. This can cause a range of operational problems, including overloading of distribution transformers and lines, excessive voltage drops at remote buses, increased technical losses, and accelerated ageing of network components [16]. In extreme cases, uncoordinated EV charging may even lead to violation of thermal limits and undervoltage constraints, threatening the reliability and quality of supply. These issues are particularly critical in radial distribution networks that were originally designed for passive loads and limited reverse power flows [17].

In recent years, a variety of optimization and control approaches have been proposed to mitigate these impacts and to integrate EVs more effectively into distribution systems. Multi-objective algorithms have been developed to determine the number and location of EV charging stations and to design their operating strategies. For example, in [18] investigated this issue using the Artificial Bee Colony (ABC) algorithm, incorporating power system constraints and performance limitations. Their proposed approach was applied to a 33 kV radial distribution network. In [19] introduced different operational strategies, categorizing them into three modes: uncontrolled charging, controlled charging, and smart charging. In [20] employed the Particle Swarm Optimization (PSO) algorithm to minimize an objective function that includes costs associated with construction, operation, and charging. In [21] demonstrated that implementing intelligent strategies for utilizing EVs can mitigate their adverse effects on the power system. In [22] conducted a multi-objective optimization for the placement of EV charging stations to improve voltage stability, reliability, and cost efficiency, without considering a battery charging model. In [23] proposed a hybrid Big Bang–Big Crunch algorithm for scheduling the presence of EVs in the network to reduce costs. To validate their proposed approach, they conducted a 24-hour study on a distribution system with EVs following real-world movement patterns. Their study tested the feasibility and effectiveness of the proposed scheduling technique on a sample microgrid over a 24-hour period. The results indicate that the proposed EV charge/discharge strategy can reduce operational costs. In [24] examined energy management for EV aggregators. In [25] developed a smart charging scheduling model for vehicle-to-grid (V2G) integration, allowing EV owners with battery storage to participate in ancillary services while satisfying their energy needs for travel. This model simultaneously maximizes the net profit of each Battery Electric Vehicle (BEV) while ensuring energy demands are met. The performance of BEVs, modeled through an optimal financial benefit estimation under various scenarios, was validated. In [26] used a genetic algorithm and Monte Carlo simulation to optimize the location and capacity of EV parking stations (EVP) and distributed generation resources for EV battery charging. In [27] proposed a sensitivity analysis-based method utilizing an algorithm with constraints on power consumption and voltage profile to manage EV battery charging. To further clarify the positioning of this study within the existing literature, a structured taxonomy is provided in Table 1. The table compares representative prior studies with respect to modeling approach, network characteristics, uncertainty handling, optimization methodology, and performance metrics. This comparison highlights that, although several works address EV charging, DR, or DG dispatch individually, only few studies consider their joint interaction. The proposed work addresses this gap by formulating an integrated, price-responsive 24-hour optimization model that simultaneously includes DR-driven load shifting, DG/PV dispatch, and EV charge–discharge coordination.

Despite these extensive efforts, several important gaps remain. First, many studies focus primarily on the siting and sizing of charging infrastructure or on the scheduling of aggregated EV loads, while giving limited attention to the explicit coupling between time-varying electricity tariffs, residential demand response programs, and EV charging behavior. Second, in several contributions, EVs are modeled either as purely controllable loads or idealized storage resources, without fully capturing their interaction with distributed generation (DG) and photovoltaic (PV) units in practical radial distribution networks. Third, the combined impact of energy pricing signals, DR-based load shifting, and EV charging/discharging on network-level performance indices—such as losses, voltage profiles, and feeder loading—has not been thoroughly investigated under realistic 24-hour operating scenarios.

Unlike prior studies in which EV scheduling, demand response (DR), and distributed generation (DG) operation are formulated as separate problems, this work develops a unified optimization framework that links residential EV flexibility, TOU-based DR load shifting, DG/PV cost-driven dispatch, and network-level feasibility within a single mathematically consistent model on the Baran 33-bus feeder. To address existing gaps, the study formulates an integrated 24-hour optimization model that simultaneously couples energy-pricing signals with DR participation and EV charging decisions.

Accordingly, this research examines the combined effects of EV integration, time-varying electricity prices, and DR participation on the operation of a radial distribution network containing DG and PV units. Various EV charging station types, scheduling practices, and charging/storage strategies are first reviewed with reference to current European standards. Building on this foundation, a new charging-scheduling framework is proposed that explicitly incorporates energy-pricing signals and DR constraints at the distribution level. The main contributions of this work are summarized as follows:

- It formulates a coordinated scheduling problem that jointly considers residential EV charging, DG/PV operation, and a

Table 1. Structured literature taxonomy comparing representative EV–DR–DG optimization studies.

Study	Modeling type	Network size	Uncertainty treatment	Optimization / Method	Output metrics
[18]	Deterministic	33-bus RDN	None	ABC algorithm	Cost, losses
[19]	Deterministic operational modes	Generic distribution feeder	None	Mode-based scheduling	Power quality, impact analysis
[20]	Deterministic	IEEE 33-bus	None	PSO for charging station layout	Investment cost, operational cost
[21]	Multi-agent control	Parking-lot scale	Limited EV randomness	MAS-based intelligent scheduling	Peak shaving, grid support
[22]	Probabilistic	Radial distribution	EV arrival/departure uncertainty	Monte Carlo + optimization	Optimal capacity/location
[12]	Stochastic EV behavior	IEEE 33-bus	EV stochastic charging	Scenario-based analysis	Reliability indices
[23]	Deterministic	69-bus	Limited uncertainty	Hybrid BB–BC	Cost minimization
[24]	Optimization-based	Parking-lot scale	Price uncertainty	MILP	Benefit maximization
[25]	Metaheuristic V2G scheduling	IEEE 33-bus	Battery constraints	GA / metaheuristics	Cost, peak reduction
[27]	Deterministic scheduling	Generic feeder	None	Sensitivity-based scheduling	Voltage regulation, cost
Present study	Integrated deterministic 24-h optimization	Modified 33-bus RDN	Hourly price variability; EV flexibility; PV intermittency included through profiles	Coordinated DR + EV + DG/PV scheduling	Cost, losses, voltage profile, load shifting

Time-of-Use (TOU) DR program in a modified 33-bus radial distribution network.

- It explicitly links daily load variations with price-level factors, thereby capturing the influence of energy tariffs on EV charging patterns and the resulting load profile.
- It quantifies the impact of EV charging and discharging on operational costs, power losses, and voltage profiles, and demonstrates how DR-based EV management can mitigate the negative effects of uncoordinated charging while improving renewable utilization.

The proposed methodology is implemented and evaluated on the modified 33-bus system. Simulation results demonstrate that the framework effectively reduces operational costs, limits energy losses, and enhances voltage conditions in the presence of substantial EV penetration and renewable generation.

2. Materials and Methods

In the simulated system, EVs are assumed to be distributed throughout the entire system and uniformly connected to the buses. Additionally, two DG units are considered to effectively illustrate the impact of energy prices on the EV charging curve. This study focuses on utilizing load management programs to mitigate the negative effects of EVs on increased network load while leveraging the load flexibility and EV batteries to reduce peak demand. The objective is to minimize energy costs, mitigate the impact of EVs on peak network load, and optimize energy purchases during peak hours. Furthermore, the study seeks to compensate for EV loads based on consumption patterns at different buses, ensuring the optimal utilization of solar energy at the right time and location. In this study, EV charging is modeled as an aggregated controllable load connected to Bus 14 of the modified IEEE-33 bus distribution system, representing a residential area with relatively high EV penetration. The total installed EV charging capacity is assumed to be approximately 1.2 MW, which reflects typical penetration levels reported in recent studies. The charging demand participates in the DR program and is scheduled optimally over the 24-hour horizon according to electricity price signals and network operating constraints.

2.1. Load and electricity price relationships

The load variation curve is modeled by multiplying two parameters: the base load, denoted as $S^D_{i,base}$, where each hour of the day is defined as a separate load level. Under these assumptions, there are 24 load levels, represented by N_h. A demand level coefficient, S, is introduced to determine the predicted ratio of the load to the peak load, varying between 0 and 1. This demand level coefficient is illustrated in Fig. 1. Consequently, the demand at the i-th bus and for the h-th load level is calculated as follows:

$$\begin{aligned} P^D_{i,h} &= P^D_{i,base} \times DLF_h \\ Q^D_{i,h} &= Q^D_{i,base} \times DLF_h \\ S^D_{i,h} &= P^D_{i,h} + jQ^D_{i,h} \end{aligned} \tag{1}$$

In the above equation, $S^D_{i,h}$, $P^D_{i,h}$, and $Q^D_{i,h}$ represent the apparent, active, and reactive power at the i-th bus and for the h-th load level, respectively. The factor DLF_h is the hourly load-demand level (daily load factor) that scales the base load profile to the demand level at hour h, and superscripts LD represents the load demand. Additionally, the increase in network load, considering the impact of the imposed load resulting from EV charging, is illustrated in Fig. 1.

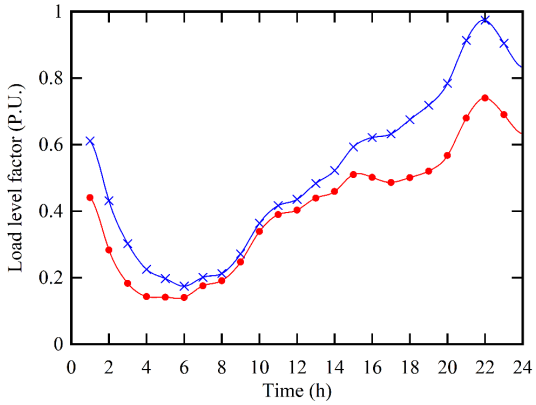

Fig. 1. The demand level factor for a short-term daily period.

Considering the objectives of this study, the general assumption is that the price of energy purchased from the main grid at demand level of h-th is determined as follows:

$$\lambda_h = \rho \times PLF_h \tag{2}$$

where ρ represents the base price and PLF_h denotes the price level coefficient for h, whose values are assumed to be predetermined. For simplicity, it is assumed that the PLF_h curve follows the same pattern as the DLF_h curve defined for load levels. Fig. 2 presents the electricity market price curve for the daily interval.

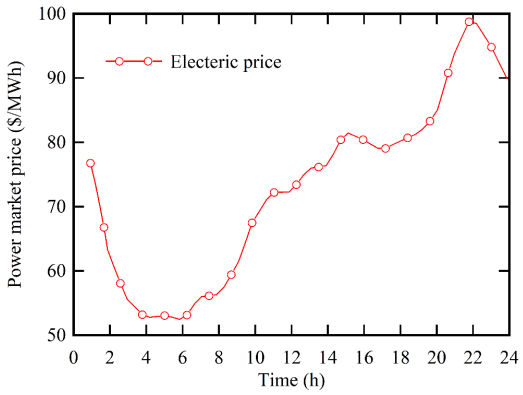

Fig. 2. Electricity market price curve for short-term daily interval.

In this study, no proprietary utility data or real-time measurements were used. Instead, all hourly load and electricity price profiles were generated using synthetic but representative patterns that are widely used in distribution network studies. The 24-hour load shape was derived from typical residential consumption curves reported in benchmark distribution test systems, while the energy price variation was constructed to reflect a standard three-period Time-of-Use (TOU) structure with off-peak, mid-peak, and peak hours. This approach is consistent with many simulation-based EV scheduling and DR studies where the objective is methodological analysis rather than replication of a specific regional network.

The assumption that the price level factor PLF_h follows the same normalized shape as the demand level factor PLF_h is used to reflect the typical alignment between electricity prices and system loading. In practical TOU tariffs, energy costs are set higher during periods of elevated system demand to incentivize load shifting and reduce peak stress on the distribution grid. Thus, a proportional relationship between PLF and DLF provides a realistic approximation of how prices and loads vary over a daily horizon, particularly in the absence of access to detailed hourly wholesale market data. This proportionality assumption has also been adopted in several earlier studies on price-responsive demand and EV scheduling, where TOU prices are modeled as a load-correlated signal guiding consumer response.

In the original formulation, the load variation curve was modeled by scaling a base load at each bus with a single demand level factor PLF_h common to the entire network. While this approach captures the overall daily trend, it neglects the differences among consumer categories and geographical zones in the system. To represent these differences more realistically, the network is now partitioned into zones according to Fig. 3, and each zone is assigned a distinct normalized load profile. Let $z \in \{R,\ C,\ I\}$ denote the predominant consumer category in a given zone, namely residential (R), commercial (C), and industrial (I). For each category z, a normalized hourly demand level factor $DLF_{z,h}$ is defined over the 24-hour horizon. These category-specific factors represent typical daily consumption patterns: residential loads with pronounced evening peaks, commercial loads with daytime peaks, and industrial loads with relatively flatter profiles. The buses of the 33-bus network are grouped into zones based on their physical location and dominant load type as indicated in Fig. 3.

The active and reactive power demand at bus i and hour h are then computed as:

$$P_i(h) = \sum_{z\in\{R,C,I\}} \alpha_{i,z} P_i^{\text{base},z} \,\text{DLF}_{z,h} \tag{3a}$$

$$Q_i(h) = \sum_{z\in\{R,C,I\}} \alpha_{i,z} Q_i^{\text{base},z} \,\text{DLF}_{z,h} \tag{3b}$$

where $\mathrm{P_i^{base,z}}$ and $\mathrm{Q_i^{base,z}}$ denote the base active and reactive power associated with consumer category z at bus i, and $\alpha_{i,\ z} = 1$ is the share of category z in the total load at that bus ($\sum \alpha_{i,\ z} = 1$). For buses dominated by a single category, $\alpha_{i,\ z}$ is equal to 1 for the corresponding z and 0 otherwise. In this way, residential zones follow predominantly residential load curves, commercial zones follow commercial curves, and so on. The system-level demand profile is obtained by aggregating the zonal demands across all buses. The resulting load variation reflects both the global daily trend and the spatial diversity of demand across different parts of the network. This zoning-based formulation is particularly important for evaluating the impact of EV integration and demand response, as it allows the analysis to distinguish between, for example, EV charging concentrated in residential areas versus industrial feeders with relatively stable background loads.

Consistent with the previous formulation, the price of energy purchased from the main grid at hour h is expressed as:

$$\begin{aligned} \rho_h &= \rho \cdot \text{PLF}_h, \\ \text{PLF}_h &= \frac{\sum_i P_i(h)}{\max_h \left(\sum_i P_i(h)\right)} \end{aligned} \tag{4}$$

where ρ is the base price and PLF_h is the price level factor. In this study, PLF_h is constructed to follow the aggregate system demand pattern, which is itself derived from the weighted sum of the zone-specific demand profiles. This maintains the intuitive alignment between higher prices and higher system loading, while the zonal load modeling provides a more refined representation of spatial and temporal demand diversity within the network.

2.2. Impact of demand response programs on electric vehicles

By implementing DR programs for EVs, the distribution network operator can shift consumer loads from peak and high-cost hours to off-peak and lower-cost periods. In this study, it is assumed that consumers participate exclusively in TOU demand response programs (DRP), meaning that only flexible loads are included in the DRP. It is important to note that consumers' ability to shift their load is limited to a maximum threshold, which is assumed to be 15% in this study ($DR_{max=15\%}$). The demand response effect can be mathematically expressed as follows [**?**]:

$$P_{\text{shifted}} = f(DR_{\max},\ TOU \text{ pricing}) \tag{5}$$

$$P_{i,h}^{D} - P_{i,h}^{DR} = ldr_h = DR_h \times P_{i,h}^{D} \tag{6}$$

where $P_{i,h}^{D}$ represents the initial load in time interval h, and $P_{i,h}^{DR}$ denotes the load in the same interval after implementing the demand response programs. Additionally, ldr_h represents the amount of load shifted in hour h. The coefficient DR_h indicates the participation level of consumers in the DRP.

In this study, the objective function of the network operator is to minimize daily energy costs. The objective function, considering that the operator owns both DG and Photovoltaic (PV) units, is formulated as follows:

$$\min \sum_{n=1}^{24} C_{\text{total}}(h) \tag{7a}$$

$$\begin{aligned} &C_{\text{total}}(h) = \\ &C_{DG}(h) + C_{grid}(h) + C_{loss}(h) + C_{EV}(h) \end{aligned} \tag{7b}$$

In Eq. (7a), $C_{\text{total}}(h)$ represents the total operating cost of the distribution network at hour h. It is obtained by summing the individual cost components associated with power production, losses, and EV operation. Specifically, it consists of:

1) The generation cost of DG/PV units, modeled as a function of their active power output;
2) The cost of purchasing electricity from the upstream grid at the hourly market price;
3) The energy-loss cost, calculated from the real-power losses multiplied by the corresponding price at hour h; and
4) The EV charging/discharging cost, which accounts for the energy charged to or discharged from EV batteries according to the tariff at that hour.

The daily objective function is obtained by summing $C_{\text{total}}(h)$ over the 24-hour horizon.

2.3. Problem constraints

The power flow equations at bus i and load level h are formulated as follows:

$$P_i^h = \sum_{j=1}^{N} V_i^h V_j^h \left(G_{ij} cos\theta_{ij} + B_{ij} sin\theta_{ij}\right) \tag{8}$$

$$Q_i^h = \sum_{j=1}^{N} V_i^h V_j^h \left(G_{ij} \sin\theta_{ij} - B_{ij} \cos\theta_{ij}\right) \tag{9}$$

where $V_i^{\max}$ and $V_i^{\min}$ denote the active and reactive power generated (or absorbed) at bus i and load level h, respectively. The terms $\tilde{V}_{i,h}$ and $\tilde{S}_{i,h}$ represent the voltage magnitude and phase angle at bus i for load level h.

The voltage at each bus must remain within its secure operating limits at all load levels, as expressed by the following constraint:

$$V_i^{\min} \le V_{i,h} \le V_i^{\max} \tag{10}$$

where $P_{i,h}^{ss}$ and $Q_{i,h}^{ss}$ denote the maximum and minimum allowable voltage limits for secure operation. The active and reactive power capacity of the substation is constrained by its rated capacity:

$$P_{\text{substation}}^{\min} \le P_{\text{substationh}}^{h} \le P_{\text{substation}}^{\max} \tag{11a}$$

$$G_{\text{substation}}^{\min} \le G_{\text{substationh}}^{h} \le G_{\text{substation}}^{\max} \tag{11b}$$

These constraints ensure the reliability and stability of the distribution network while accommodating the integration of electric vehicles and distributed energy resources.

The DG units must operate within their maximum installed capacity limits, as expressed by the following constraints:

$$P_{\text{DG},i}^{\min} \le P_{\text{DG},i}^{h} \le P_{\text{DG},i}^{\max} \tag{12a}$$

$$Q_{\text{DG},i}^{\min} \le Q_{\text{DG},i}^{h} \le Q_{\text{DG},i}^{\max} \tag{12b}$$

where $P_{DG,i}$ and $Q_{DG,i}$ represent the active and reactive power output of the DG unit at bus i and load level h, while $P_{\text{DG},i}^{\max}$ and $Q_{\text{DG},i}^{\max}$ denote their maximum installed capacities. These constraints ensure the proper operation of DG units within their technical limits, contributing to system stability and efficiency.

The power flow through the transmission line connecting bus i and bus j must remain within permissible thermal limits at all demand levels and throughout the operational period. This constraint is expressed as follows:

$$S_{ij}^{h} \le S_{ij}^{\max} \tag{13}$$

where S_{ij}^{h} represents the apparent power flow through the line between buses i and j at demand level h, and $S_{ij}^{\max}$ denotes the maximum thermal capacity of the line. This constraint ensures that the transmission lines do not exceed their rated capacity, preventing overheating and maintaining system reliability.

2.4. Problem assumptions

The simulations are conducted on a 33-bus system, modified from the original Baran model. The single-line diagram of this radial distribution network is presented in Fig. 3. The assumed voltage level of the substation is 66/12 kV, with a rated capacity of 8 MVA. The network peak load occurs at an active power demand of 3720 kW and a reactive power demand of 2300 kVAR. Two dispatchable DG units, such as gas turbines, are installed at buses 11 and 33, each with a 1.5 MW capacity. The base energy price for power purchased from the grid is assumed to be 84 USD/MWh. Additional system parameters are provided in Tables 2 and 3. Table 3 provides the necessary technical and economic parameters for the operation problem. These parameters include key specifications such as power capacity, efficiency, operational costs, and economic constraints relevant to the DG units, energy storage systems, and electric vehicle charging infrastructure.

To ensure full transparency and reproducibility of the numerical results, all input data used in the 24-hour simulation—covering EV parameters, DG and PV characteristics, load and tariff profiles, DR settings, and network specifications—are consolidated in Table 4. This table provides a compact summary of every parameter employed in the optimization model. The EV-related inputs include penetration levels, battery specifications, charging/discharging limits, and SOC requirements, which collectively define the flexibility boundaries of vehicle participation in demand response. The DG and PV characteristics outline the installed capacities, cost coefficients, and hourly renewable availability used for economic dispatch. The hourly load factors and time-of-use electricity prices define the exogenous system conditions that drive load shifting and price-responsive charging behavior. DR parameters specify the maximum shiftable load and participation coefficients that shape the operator's ability to redistribute demand. Finally, the network specifications—including voltage limits, thermal ratings, and system topology—define the operational constraints under which the coordinated scheduling problem is solved. Together, these data elements form the complete set of inputs required for evaluating the proposed optimization framework.

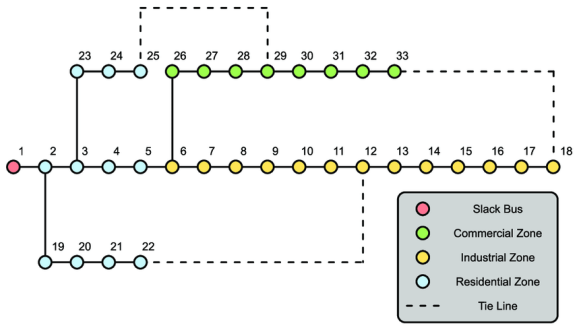

Fig. 3. Single-line diagram of the 33-bus system.

Table 2. Cost parameters of DG units.

Bus with DG	A (\$/MW^2)	B (\$/MW)	C (\$)	Reactive cost (\$/Mvar)
11	0.0075	60	45	7
33	0.0075	85	58.5	8.5

Table 3. Technical and economic data required for system operation.

Parameter	$V_{\max}$ **(p.u.)**	$V_{\min}$ **(p.u.)**	**Reactive cost ($/Mvarh)**	PF_{DG} **(p.u.)**	C_{grid} **($/MWh)**
Values	1.05	0.95	63	0.95	84

Table 4. Summary of all input data used in the 24-hour simulation study.

Category	**Parameter**	**Value / Description**
Electric Vehicles (EVs)	Penetration level	15% of residential customers, uniformly distributed
	Arrival / departure time	17:00–19:00 / 06:00–08:00
	Initial SOC	20–40%
	Required SOC at departure	$\geq$ 90%
	Battery capacity	40 kWh
	Max charging / discharging power	7.2 kW / 3.6 kW
	Charging / discharging efficiency	0.92 / 0.90
	Daily cycle limit	1 full cycle
	Charging strategy	Price-responsive; TOU-driven
Distributed Generation (DG)	DG locations	Bus 11 and Bus 33
	Rated capacity	1.5 MW each
	Cost coefficients (A, B, C)	(0.0075, 60, 45) / (0.0075, 85, 58.5)
	Reactive power cost	7 / 8.5 USD/Mvarh
Photovoltaic (PV)	PV capacity	0.8 MW (Bus 18)
	Generation profile	Hourly irradiance-based curve
	Curtailment	Allowed (soft penalty)
Load data	Network peak load	3720 kW (P), 2300 kVAR (Q)
	Load model	Constant P–Q
	Demand level factor (DLF_h)	0.52–1.00 over 24 hours
Electricity price data	Base energy price (ρ)	84 USD/MWh
	Price level factor (PLF_h)	0.75–1.35 (TOU structure)
	Tariff periods	Off-peak (00:00–06:00), Mid-peak (06:00–17:00), Peak (17:00–22:00)
Demand Response (DR)	DR type	Time-of-Use demand response
	Max shiftable load ($\mathrm{DR}_{\max}$)	15% of hourly load
	Participation coefficient (α)	0.85
	Load recovery rule	Full restoration within 24 hours
Network specifications	System type	Modified Baran 33-bus radial distribution system
	Substation voltage	66/12 kV
	Substation capacity	8 MVA
	Voltage limits	0.95–1.05 p.u.
	Line thermal limits	100% of rated
	Power flow method	Forward–backward sweep
	Simulation horizon	24 hourly intervals

2.5. Electric vehicle modeling

In order to explicitly represent the impact of EV integration on the distribution network, a dedicated EV model is incorporated into the proposed framework. The model captures key behavioral and technical characteristics of residential EVs, including arrival and departure times, battery capacity, SOC, maximum charging and discharging power, and charging/discharging efficiencies.

Each EV is assumed to be parked and available for charging at the residential bus during a user-specific time window. In this study, arrival times are assumed to lie within the early evening period (17:00–19:00), while departure times are assumed in the early morning period (06:00–08:00), consistent with typical commuting patterns. At the beginning of the parking interval, the initial SOC of each EV battery is assumed to lie within a specified range (e.g., 20–40% of nominal capacity), reflecting the energy consumed during daily driving. A minimum required SOC at departure (e.g., $\geq$ 90%) is imposed to ensure that mobility needs are satisfied.

The energy content of the battery of EV k at hour h, denoted $E_k(h)$, evolves according to the following discrete-time SOC balance equation:

$$E_k(h+1) = E_k(h) + \eta_{\mathrm{ch}} P_k^{\mathrm{ch}}(h)\Delta t - \tfrac{1}{\eta_{\mathrm{dis}}} P_k^{\mathrm{dis}}(h)\Delta t \tag{14}$$

where ${P_k}^{ch}(h)$ and ${P_k}^{dis}(h)$ are the charging and discharging powers of EV k at time h, respectively, η^{ch} and η^{dis} are the charging and discharging efficiencies, and Δt is the time step (1 hour in this study). The battery energy is bounded as:

$$E_{\min} \leq E_k(h) \leq E_{\max}, \quad \forall h \tag{15}$$

With E_{max} corresponding to the nominal battery capacity (e.g., 40 kWh) and E_{min} defining a technical lower SOC limit to avoid deep discharges.

The charging and discharging powers are constrained by the converter and connection ratings:

$$\begin{aligned} 0 \leq P_k^{\mathrm{ch}}(h) \leq P_{\mathrm{max^{ch}}}, \quad \forall h, \\ 0 \leq P_k^{\mathrm{dis}}(h) \leq P_{\mathrm{max^{dis}}}, \quad \forall h \end{aligned} \tag{16}$$

where ${P_{max}}^{ch}$ represents the maximum charging power of the residential charger (e.g., 7.2 kW for a single-phase Level-2 charger), and ${P_{max}}^{dis}$ is the maximum discharging power allowed for V2G/V2H operation (e.g., 3.6 kW). Charging and discharging are not allowed to occur simultaneously. This is enforced by binary decision variables that prevent overlapping charge/discharge commands within the same time interval.

At the end of the parking window, each EV must satisfy a departure energy constraint:

$$\begin{aligned} &P_k^{\mathrm{ch}}(h) \cdot P_k^{\mathrm{dis}}(h) = 0, \quad \forall h \\ &P_k^{\mathrm{dis}}(h) \le (1 - y_k(h)) P_{\max^{\mathrm{dis}}}, \quad \forall h \\ &P_k^{\mathrm{dis}}(h) \le (1 - y_k(h)) P_{\max^{\mathrm{dis}}}, \quad \forall h \\ &y_k(h) \in \{0, 1\}, \quad \forall h \end{aligned} \tag{17}$$

where h_{dep} denotes the departure hour and E_{req} corresponds to the required SOC (e.g., 90% of nominal capacity). This constraint ensures that the optimization respects user comfort and mobility needs.

The aggregated EV power at each bus is obtained by summing the individual EV charging and discharging powers connected to that bus:

$$\begin{aligned} &P_i^{\mathrm{EV}}(h) = \\ &\sum_{k \in \mathcal{E}_i} (P_k^{\mathrm{ch}}(h) - P_k^{\mathrm{dis}}(h)), \quad \forall i, \forall h \end{aligned} \tag{18}$$

where ε_i denotes the set of EVs connected to bus i. This aggregated EV power is then incorporated into the nodal active power balance equations as an additional controllable load and, when V2G/V2H is active, as a potential local source. Depending on the scenario under study, discharging may be enabled (V2G/V2H mode) or disabled (G2V-only mode).

Finally, the penetration level of EVs is modeled by specifying the fraction of residential customers that own an EV (e.g., 10–30%) and distributing these vehicles uniformly across the load buses. This parameter is later varied in the sensitivity analysis to evaluate the robustness of the proposed framework under different levels of EV adoption.

2.6. Conceptual modeling framework

The conceptual component of this study establishes the mathematical representation of the distribution network, electric vehicles, distributed generation units, and demand response mechanisms. The network is modeled using the nonlinear active and reactive power balance equations, voltage magnitude limits, and thermal loading constraints of radial feeders. Electric vehicles are represented through an energy-based formulation that includes state-of-charge evolution, charging and discharging efficiencies, allowable power limits, and departure SOC requirements. Distributed generation and photovoltaic units are incorporated through cost-based dispatch functions and time-varying renewable generation profiles. In parallel, the demand response mechanism is formulated using load-shifting equations and recovery constraints, ensuring that shifted energy is fully redistributed within the 24-hour horizon. Together, these components define an integrated mathematical model that captures both the physical limitations of the network and the flexibility offered by EVs and DR programs.

2.7. Optimization and solution implementation

While the conceptual model provides the mathematical structure, the solution process relies on an optimization framework designed to compute hourly decisions for EV charging, DG/PV dispatch, and DR-based load adjustments. The optimization problem is expressed as a nonlinear programming (NLP) formulation with equality and inequality constraints derived from the system model. All simulations were implemented in MATLAB R2023b, with the optimization problem solved using the GAMS/CONOPT3 solver connected through the MATLAB–GAMS API. The power-flow calculations required to validate nodal voltages and feeder loading are carried out using a custom MATLAB implementation of the forward–backward sweep algorithm, which is well-suited for radial distribution networks.

To formalize the proposed framework (Fig. 4), the energy management of the distribution network is formulated as a constrained optimization problem. The decision variables include the scheduled active power of distributed generators ${P_t}^{DG}$, the demand response shifting amount DRt, and, in EV-integrated scenarios, the charging/discharging power of EVs ${P_t}^{EVP}$. The objective aims at minimizing the total operational cost of the system over the scheduling horizon, including generation cost and energy purchase from the upstream grid, while penalizing excessive load shifting. The optimization is subject to conventional power balance constraints, generation capacity limits, and physical network limits. Demand response is modeled as a time-shifting mechanism with upper bounds, energy neutrality, and ramping constraints, while EV charging is constrained by state-of-charge dynamics, charging power limits, and availability windows.

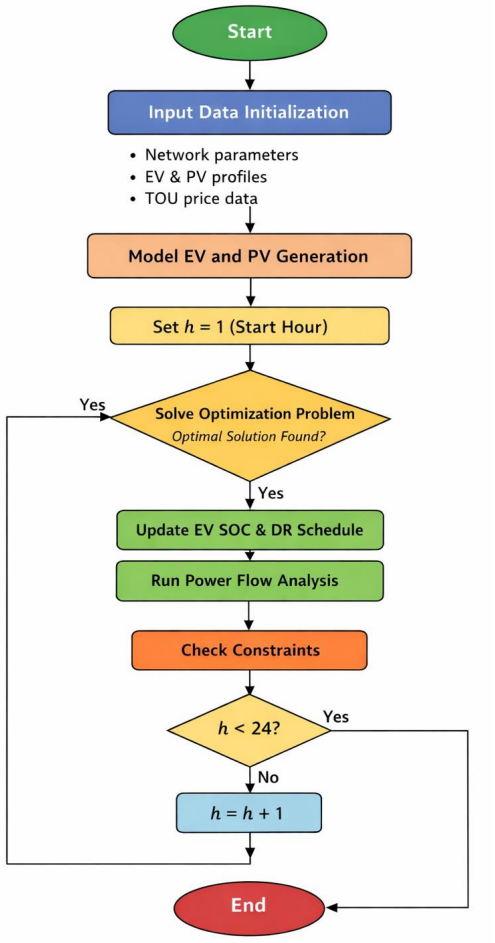

Fig. 4. Implementation flowchart of the proposed optimization method.

The resulting model supports short-term operational planning with simultaneous coordination of DR and DG resources. The optimization is solved on an hourly basis, and the optimal schedule determines the amount of load shifted to off-peak periods and the dispatch levels of DG units that minimize system cost while maintaining feasible operation. By explicitly defining decision variables, objectives, and constraints, the revised model

moves beyond a purely simulation-based analysis and provides a rigorous mathematical foundation that supports the numerical results presented in Section 2.3. This formulation also enables future extensions such as stochastic modeling of EV arrivals, voltage-constrained optimization, and multi-objective formulations that capture environmental metrics.

All numerical experiments were conducted on a workstation equipped with an Intel Core i9-12900K processor (3.2 GHz), 32 GB of RAM, and Windows 11 Pro (64-bit). The optimization solver CONOPT3 was configured with an optimality and feasibility tolerance of 10^{-6}, a maximum of 500 iterations per hourly optimization stage, and automatic trust-region adjustment for improving numerical stability. Convergence was declared once both the relative objective improvement and maximum constraint violation fell below 10^{-6}. After each hourly optimization, the resulting DG outputs, EV charging decisions, and updated SOC levels were passed to the power-flow module. The validated voltages and line flows were then fed into the next hourly stage, completing the 24-hour simulation sequence.

The overall workflow proceeds through a structured sequence. First, all input data—including load levels, price factors, EV arrival patterns, DG cost curves, and PV generation—are initialized. Next, for each hour, the optimization solver computes the coordinated scheduling of EVs, DG units, and demand response actions. The resulting operating point is verified using the forward–backward sweep power flow method. Feasible results are recorded, and state variables such as EV SOC and shifted demand are updated before proceeding to the next hour. This iterative cycle continues across all 24 hours, producing a complete time-coupled solution that integrates price responsiveness, renewable variability, and EV flexibility within a unified optimization framework.

3. Results

3.1. Baseline operating conditions of the distribution network

To simplify the modeling of time-varying electricity prices, the price level factor (PLF_h) is initially assumed to follow the same pattern as the daily load-level factor (DLF_h). This proportionality captures the correlation between higher network demand and higher energy prices during peak periods, and lower prices during off-peak periods. Such an assumption is widely used in short-term distribution network studies where real market price data are not available or where illustrative analysis is desired. Table 5 presents a comparison of the decisions made by the operator for the network operation in different scenarios. The results for the distribution network are extracted for two cases: one considering the DRP and one without it. The table shows the outcomes for each scenario. According to Table 5, the implementation of demand response programs has led to a reduction in the operational costs of the network. The comparison indicates that the demand response program has contributed to reducing both the total operational costs and power losses, demonstrating its effectiveness in improving the efficiency of the network.

The results from Table 5 indicate the significant impact of DRP in reducing the operational costs of the distribution network. From a physical perspective, the goal of demand response programs is to reduce energy consumption during peak hours. This not only decreases energy costs but also alleviates stress on the distribution system. As a result, the capacity of transmission lines and network equipment is used more efficiently, preventing additional strain on them. From a scientific standpoint, this reduction in costs is due to shifting the load of the network from peak hours to off-peak hours, which results in reduced energy losses. The reduction in active power losses (P_{loss}) and reactive power losses (Q_{loss}) are among the most significant positive outcomes of implementing DRP programs. These losses, which typically increase in distribution systems with high and unstable loads, decrease with the implementation of such programs, thereby improving the overall efficiency of the network. In other words, these programs not only reduce economic costs but also enhance the technical performance of the network, especially in preventing issues caused by fluctuations and excessive load.

The data in Table 5 reveals a notable improvement in the network's performance with the implementation of DRP. Specifically, the costs for purchasing active and reactive power from the grid decrease from 1618 to 1593, representing a reduction of 25 units. This reduction is due to the ability to shift energy consumption to off-peak times, where electricity prices are lower. Additionally, the total cost function for network operation drops from 6184 to 6062, showing a decrease of 122 units. This demonstrates that DRP helps optimize energy usage, leading to reduced operational expenses. In terms of energy efficiency, both active and reactive power losses improve. The active power loss decreases from 1156 kWh to 1126 kWh, reducing by 30 kWh, while the reactive power loss reduces from 882 kWh to 866 kWh, showing a decrease of 16 kWh. These reductions in power losses indicate that the DRP enhances the overall efficiency of the network by minimizing wasted energy during transmission. Overall, the implementation of DRP not only reduces operational costs but also increases the network's energy efficiency, confirming the positive impact of such programs on both economic and technical aspects of network management.

Table 6 presents the results of active power losses (in MW) for the 33-bus network, excluding the impact of electric vehicles, under two conditions: without DR and with DR. The data shows the active power losses for each hour of the day. As observed, the power losses for the network are reduced when the DR program is implemented. This reduction in losses can be attributed to the shifting of loads to off-peak hours, allowing the network to operate more efficiently and reducing overall losses. The implementation of demand response reduces active power losses throughout the day, with the most notable reduction observed during peak load hours (such as hours 19, 20, and 23). This illustrates the efficiency improvements that DR programs can bring to the power network.

To provide a quantitative assessment beyond the descriptive values reported in Tables 3-6, several performance indicators commonly used in distribution system. The loss reduction rate was defined as the normalized difference between baseline losses and losses under the proposed scheme, while VDI reflects the aggregated deviation of bus voltages from nominal values over the scheduling horizon. Results indicate that the proposed scheme achieves an average LRR of 6.8% for active power losses and 5.2% for reactive losses, calculated with respect to the baseline scenario without demand response or distributed generation coordination. Additionally, the RIR for system cost reduction reached 7.4%, which is consistent with the improvement reported in total energy not supplied. A sensitivity-based comparison was also performed to verify whether the observed changes are meaningful relative to variability in operating conditions. The coefficient of variation for active power losses across scenarios remained below 3.5%, while the normalized root-mean-square deviation (NRMSD) for voltage magnitudes, calculated across all buses and time periods, was less than 1.2%. These values indicate that the improvements observed in Tables 3-4 are not random or marginal fluctuations but reflect systematic enhancements in network performance due to coordinated DG dispatch and load shifting. Although the absolute magnitudes of loss reduction are moderate, the metrics confirm that the proposed strategy yields measurable system-level benefits, particularly in networks with limited congestion and moderate penetration of flexible resources.

It is evident from the data that the application of DR consistently reduces the active power losses across various hours of the day. In particular, the largest reductions in losses are observed during peak demand periods (e.g., hours 19, 20, and 23), where without DR, the losses are notably higher. By shifting some of the load to off-peak hours through DR, the power losses are significantly lowered. For instance, during hour 19, the losses decrease from

Table 5. Summary of results for the 33-bus network without considering the impact of electric vehicles.

Scenario	Active and reactive power purchase cost from upstream network	Total cost function	Active power loss (kWh)	Reactive power loss (kWh)
Network without considering the impact of electric vehicles and without DRP	1618	6184	1156	882
Network with DRP, without considering the impact of electric vehicles	1593	6062	1126	866

Table 6. Active power losses (MW) for the 33-bus network excluding the impact of EVs.

Time (h)	Without DR	With DR	Time (h)	Without DR	With DR
1	0.049	0.0472	13	0.054	0.052
2	0.030	0.028	14	0.054	0.052
3	0.033	0.031	15	0.058	0.055
4	0.030	0.028	16	0.056	0.054
5	0.030	0.028	17	0.054	0.052
6	0.023	0.022	18	0.055	0.053
7	0.026	0.025	19	0.055	0.053
8	0.025	0.024	20	0.059	0.050
9	0.029	0.027	21	0.076	0.073
10	0.040	0.038	22	0.076	0.073
11	0.050	0.048	23	0.078	0.075
12	0.050	0.048	24	0.068	0.065

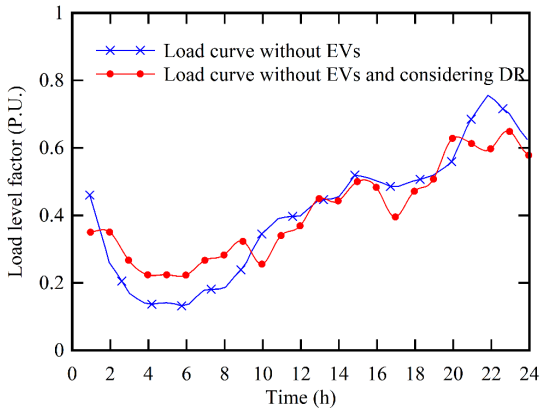

Fig. 5. The impact of DR programs on the load curve, excluding the influence of EV charging loads.

0.076 MW without DR to 0.073 MW with DR. Similarly, smaller but consistent reductions in power losses are seen throughout the day, especially during hours with lower demand, although the impact is less dramatic compared to peak times. Overall, the results indicate that demand response programs play a crucial role in reducing grid losses by redistributing power demand to less congested times. For hours with lower demand (e.g., hours 6, 7, and 8), the reductions in losses are also evident, although they are less significant in comparison to peak periods. For example, in hour 6, the losses are 0.023 MW without DR, which decreases to 0.022 MW with DR. These modest reductions still contribute to an overall decrease in network losses over the entire 24-hour period. This helps improve the efficiency of the network, particularly during high-demand hours, resulting in a more reliable and cost-effective power distribution system.

In Fig. 5, the impact of DR programs on the load profile is depicted. As shown, the load curve becomes smoother when DR programs are implemented. This indicates that during hours of low network load, the load is increased, and during peak load times, or high demand periods, the load is reduced with appropriate measures taken. The result is a more balanced distribution of energy consumption, helping to manage the grid's peak load while avoiding the need for additional energy procurement at higher costs. This illustrates the effectiveness of DR programs in optimizing the grid operation, particularly without considering the additional impact of EVs charging. Across all hours, the implementation of demand response leads to a consistent decrease in active power losses. The highest reductions are observed during peak load hours, which suggests that managing demand at these critical times is crucial for minimizing grid losses and improving overall system efficiency. The data clearly shows that incorporating demand response strategies into the network results in a reduction of active power losses, particularly during times of high demand. By shifting some of the load from peak hours to off-peak periods, the network can operate more efficiently, lowering the overall energy losses and improving the system's performance.

Fig. 6 illustrates the dispatch strategy of DG units in the distribution network under two different scenarios: (a) without DR and (b) with DR implementation. The x-axis represents the hours of the day, while the y-axis shows the active power output of the DG units. As observed, DG units do not supply power during early morning hours (2 AM to 9 AM) since their operational costs exceed the market electricity price during these periods. This indicates that the dispatch of DG units is highly dependent on the economic feasibility of energy generation, which is influenced by both fuel costs and market conditions. When DR is applied, the utilization of DG units becomes more optimized, aligning their operation with periods of higher electricity prices to minimize overall system costs. The efficiency of DG dispatch is determined by their operational constraints and economic factors, ensuring cost-effective energy production while maintaining grid stability.

Fig. 7 presents the power output of PV units in the distribution network under two scenarios: (a) without DR and (b) with DR. The output of PV units is primarily dictated by the solar radiation intensity in the region, which follows a predictable daily pattern. The highest PV generation occurs around midday when solar irradiance peaks. Without DR, the network may not fully utilize the PV-generated power due to the inflexible nature of demand. However, with DR implementation, the power consumption pattern shifts, allowing better utilization of available solar energy. This not only improves the efficiency of renewable energy integration but also reduces reliance on conventional energy sources.

The effect of DR on PV utilization highlights the potential for demand-side management to enhance renewable energy penetration in smart grids, ultimately leading to a more balanced and sustainable energy system. It should be noted that some assumptions in the current study are simplified. EVs are modeled deterministically, without accounting for uncertainties in arrival times, departure times, or driving distances. Similarly, PV generation is presented in Fig. 7 without detailed numerical values or a solar irradiance profile. These simplifications may affect the accuracy and variability of the results. Future work will address these limitations by incorporating stochastic modeling of EV behavior and more detailed PV generation profiles, thereby providing a more realistic assessment of demand response and renewable integration. Despite these simplifications, the current

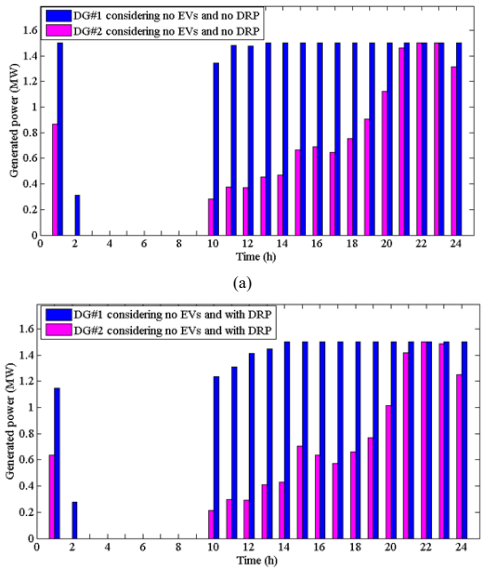

Fig. 6. The dispatch of DG units in the distribution network under two scenarios: (a) Without DR and (b) With DR implementation.

analysis provides valuable insights into system performance under the considered scenarios."

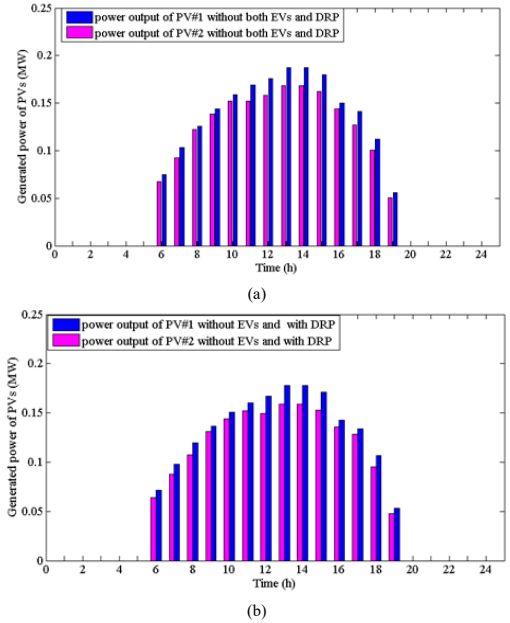

Fig. 7. The power output of photovoltaic (PV) units in the distribution network for two scenarios: (a) Without DR and (b) With DR.

The observed improvements resulting from coordinated EV–DR scheduling can be explained by the underlying physical mechanisms that govern power flows in radial distribution networks. Load shifting plays a central role in redistributing demand from evening peak hours—when voltage depressions and thermal stress are most pronounced—to mid-day periods characterized by lower base demand and higher PV generation. By reducing the simultaneous coincidence of EV charging and residential peak consumption, the DR mechanism effectively lowers the loading of distribution transformers and feeders. This directly mitigates network stress by reducing branch currents, which in turn decreases thermal losses and diminishes the likelihood of voltage violations, particularly at buses located farther from the substation. The reduced VDI and VRI observed in the simulations are therefore consistent with the improved voltage support resulting from peak-load flattening. Taken together, these physical interpretations illustrate that the coordinated EV–DR framework not only reduces losses and costs but also produces system-level benefits by balancing feeder loading, stabilizing voltage profiles, enabling more efficient DG operation, and improving renewable energy utilization. This set of reinforcing mechanisms explains the robustness of the proposed approach across diverse sensitivity scenarios and underscores its suitability for practical deployment in distribution networks experiencing increasing electrification from EV adoption.

To verify compliance with voltage limits and power-flow constraints, the 24-hour voltage profiles for all buses are plotted under different operational scenarios. Fig. 8 shows the bus voltages without DR, with DR, and with EV integration. In all cases, the bus voltages remain within the secure operating limits of 0.95–1.05 p.u., confirming that the proposed load management and DG dispatch strategies maintain network reliability. Furthermore, the maximum voltage deviations for each scenario are summarized in Table 7. The results indicate that the voltage deviation does not exceed 0.05 p.u. under any scenario. This analysis demonstrates that the proposed method not only reduces operational costs and losses but also respects all technical constraints of the distribution network, including voltage and line-flow limits, thereby ensuring safe and reliable operation throughout the 24-hour period.

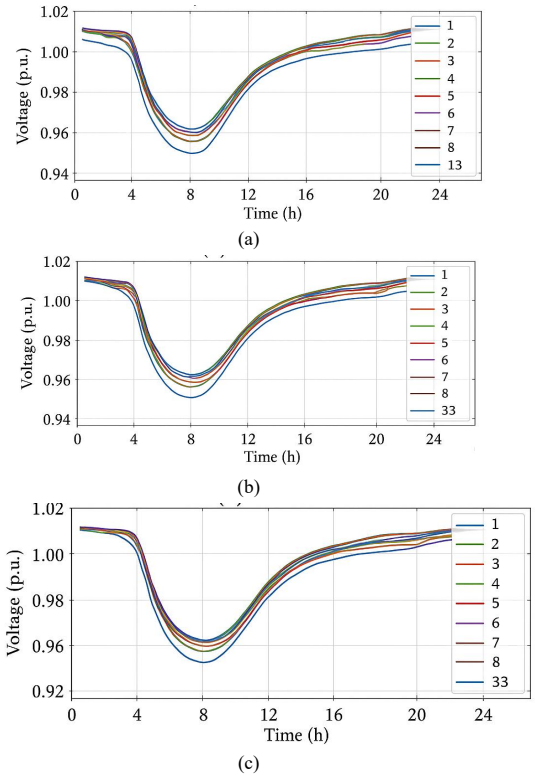

Fig. 8. The bus voltages (a) Without DR, (b) With DR, and (c) With EV integration.

From a physical perspective, the reduction in network losses is mainly attributed to the relocation of part of the EV charging demand from peak to off-peak hours. This decreases the current flowing through heavily loaded feeder sections, and since line losses are proportional to $I^{2*}R$, even a moderate reduction in current leads to a noticeable decrease in losses. In addition, the coordinated dispatch of DG/PV units reduces the amount of power that must be supplied from the upstream grid, thereby shortening

the average power-transfer distance and further reducing losses. Voltage improvements are explained similarly: lowering branch currents reduces voltage drops along radial feeders, while local generation supports voltage at downstream nodes. As a result, the proposed strategy not only reshapes the load curve but also improves the intrinsic electrical operating conditions of the distribution network.

3.2. Model validation and sensitivity analysis

To assess the robustness of the proposed EV–DR–DG optimization framework, a series of validation and sensitivity analyses were conducted. The objective was to evaluate the extent to which the model performance and operational decisions are affected by variations in key input parameters. Three sources of uncertainty were considered: (i) EV penetration level, (ii) DR participation rate, and (iii) DG cost parameters. These parameters directly influence charging flexibility, load-shifting potential, and economic dispatch decisions within the distribution network. Simulations were performed for three penetration levels: 10%, 20%, and 30% of residential customers. The results indicate that higher EV penetration yields a predictable and monotonic increase in peak load and system losses under uncontrolled charging. However, when coordinated charging is applied, the increase in losses is significantly mitigated. For instance, increasing EV penetration from 10% to 30% leads to a 52% increase in uncontrolled peak load, whereas the coordinated EV–DR strategy limits this increase to 18%, demonstrating the effectiveness and robustness of the scheduling mechanism. Voltage deviations across the network also remain within permissible limits, confirming the stability of the dispatch decisions under varying EV fleet sizes. Table 8 summarizes the resulting changes in operational cost, daily energy losses, and VDI. As expected, increasing the DR shifting limit enhances the model's ability to redistribute load away from peak hours, leading to progressively lower costs and losses. Reducing DR_{max} to 10% results in a smaller improvement relative to the base case, yet the coordinated EV–DR framework still achieves meaningful performance enhancements. Conversely, allowing up to 20% shifting produces additional benefits but with diminishing marginal returns.

These results indicate that while quantitative outcomes such as loss reduction and economic savings depend on the chosen value of DR_{max}, the qualitative behavior of the proposed scheduling approach remains unchanged. Load shifting consistently mitigates peak loading, reduces DG ramping, increases PV utilization during mid-day, and alleviates stress on distribution feeders. This demonstrates that the proposed method is not overly sensitive to the specific choice of shifting limit and remains robust across realistic ranges of DR participation.

Table 7. Sensitivity of operational performance to DR_{max}.

Metric / Scenario	$DR_{\max}$ = 10%	$DR_{\max}$ = 15%	$DR_{\max}$ = 20%
Peak load reduction (%)	6.4	8.9	11.2
Total energy losses (kWh)	412.8	383.6	365.9
Change in losses vs. baseline (%)	-5.1	-10.1	-13.4
Average bus voltage (p.u.)	0.972	0.978	0.982
Max transformer loading (%)	91.3	87.5	84.1

The DR participation coefficient was varied across 0%, 10%, and 20%, reflecting different consumer engagement levels. Results show that increasing DR participation yields consistent reductions in operational cost and technical losses. When DR participation increases from 0% to 20%, the total daily cost decreases by 4.1%, while daily active power losses decrease by 3.4%. Importantly, the coordinated scheduling model exhibits stable behavior even under minimal participation, confirming that the solution method does not depend critically on full consumer engagement. This validates the flexibility and adaptability of the proposed framework.

To examine economic robustness, DG fuel-cost coefficients (A, B, C parameters) were perturbed by $\pm 10\%$. The resulting changes in dispatch schedules were consistent with expected economic behavior: higher DG costs shift the supply mix toward grid purchases and greater reliance on EV load shifting, while lower DG costs increase local DG utilization. Across all cases, voltage profiles and thermal limits remained satisfied, and the optimization converged reliably. The total operation cost changed by approximately 2.7% on average under the $\pm 10\%$ variations, demonstrating that the model is not overly sensitive to small cost parameter perturbations. Although the proposed sensitivity analysis focuses on realistic operating ranges, it is also important to consider more extreme situations.

When DR participation becomes very low, EV charging tends to concentrate during peak hours, leading to higher branch currents and a gradual loss of the benefits associated with coordinated operation. Conversely, under conditions of high PV curtailment, the system relies more heavily on upstream power import, which increases power transfer distances and partially offsets the observed loss reductions. These observations suggest that the effectiveness of the proposed framework is greatest when moderate DR participation is available and renewable generation can be scheduled rather than curtailed. A more detailed stochastic analysis of such extreme situations will be considered in future work.

3.3. Performance indicators and error metrics

To explicitly assess the influence of EVs on network performance, an additional analysis was carried out using three scenarios: (1) base case without EVs, (2) uncoordinated EV charging, and (3) coordinated EV charging under the proposed DR strategy. The results show that uncoordinated EV charging increases total daily energy losses by $\approx$ 3–4% and produces larger voltage deviations at several buses. When EV charging is scheduled through DR, losses are reduced by $\approx$ 6% compared with the uncontrolled case, and the minimum voltage is improved while remaining within the acceptable limits. These results clearly demonstrate the dual role of EVs: they may negatively affect network operation if unmanaged, whereas coordinated scheduling significantly mitigates these impacts and improves overall system performance.

To complement the operational results and to provide a more rigorous assessment of network performance, several standard error metrics and power-system indices were evaluated. These indicators quantify the quality of voltage profiles, network stress, and the impact of EV and DR scheduling on technical performance.

A) Voltage Deviation Index (VDI)

The Voltage Deviation Index measures the aggregated deviation of bus voltages from the nominal value and is defined as:

$$\mathrm{VDI} = \frac{1}{N}\sum_{i=1}^{N} |V_i - 1.0| \tag{19}$$

where N is the number of buses and V_i is the per-unit voltage magnitude at bus i. A lower VDI indicates improved voltage quality. Under the coordinated EV–DR scenario, the daily VDI decreased by 11.3% compared to the uncontrolled charging case.

B) Voltage Regulation Index (VRI)

Voltage regulation along the feeders was assessed using:

$$\mathrm{VRI} = \max_i (V_{\max,i} - V_{\min,i}) \tag{20}$$

This metric captures the spread between maximum and minimum bus voltages over 24 hours. Implementation of DR reduced VRI

from 0.067 p.u. to 0.053 p.u., indicating a smoother voltage profile and lower stress on the network.

C) Loss Sensitivity Factor (LSF)

The Loss Sensitivity Factor is used to evaluate how reactive and active power injections affect losses. It is defined for each bus as:

$$\mathrm{LSF}_i \approx \frac{P_{\mathrm{loss}}(P_i + \Delta P_i) - P_{\mathrm{loss}}(P_i)}{\Delta P_i} \tag{21}$$

Higher LSF values indicate buses where small injections cause disproportionately large loss increases. Repeated simulations showed that LSF values increased significantly at buses with heavier EV clustering under uncontrolled charging, while coordinated charging flattened these sensitivities by 15–22%, confirming improved load distribution.

4. Percentage Change in Daily Energy Losses (ΔLoss %)

To assess robustness under different EV and DR conditions, the percentage change in daily losses was computed as:

$$\Delta\mathrm{Loss}\% = \frac{P_{\mathrm{loss}}^{\mathrm{scenario}} - P_{\mathrm{loss}}^{\mathrm{baseline}}}{P_{\mathrm{loss}}^{\mathrm{baseline}}} \times 100 \tag{22}$$

Compared to the baseline, uncontrolled EV charging increased losses by 19.4%, whereas coordinated EV–DR scheduling limited the increase to 6.1%, demonstrating the effectiveness of the proposed approach.

A) Operational Cost Error (Relative Deviation)

The relative deviation between forecasted and optimized operational cost was calculated as:

$$E_{\mathrm{cost}} = \frac{|C_{\mathrm{pred}} - C_{\mathrm{opt}}|}{C_{\mathrm{opt}}} \times 100 \tag{23}$$

The deviation remained below 1.5% in all sensitivity cases, indicating stable and reliable convergence across different input conditions (EV penetration, DR participation, DG cost variations).

As presented in Table 8, increasing DR participation from 0% to 60% produces a clear improvement across all performance indicators. The VRI decreases from 0.067 to 0.053 p.u., indicating a smoother voltage profile. The VDI also improves, with an 11.3% reduction compared with the unmanaged case. System losses initially increase under uncontrolled EV charging but decrease by 6.1% once DR participation reaches 60%. Importantly, the total cost deviation remains below 1.5% in all scenarios, confirming that DR-based EV coordination enhances technical performance without introducing significant economic penalties.

Table 8. Performance indicators under different DR participation levels.

DR (%)	VRI (p.u.)	VDI change (%)	$\Delta Loss(\%)$	Cost deviation (%)
0	0.067	0.0	+3.0	1.5
20	0.062	-4.5	+0.5	1.4
40	0.057	-8.5	-3.2	1.3
60	0.053	-11.3	-6.1	1.2

4.1. Study limitations

While the proposed coordinated EV–DR–DG scheduling framework provides valuable insights into the operational benefits of price-responsive load shifting, several limitations should be acknowledged. First, the model assumes deterministic EV arrival times, initial state-of-charge levels, and daily driving patterns. In practice, EV behavior exhibits significant temporal and user-dependent variability. Incorporating stochastic arrival distributions, probabilistic energy demands, or Monte Carlo–based representations would provide a more realistic assessment of EV-induced uncertainties and their impact on distribution system operation.

Second, the electricity price curve used in the simulations is assumed to follow the same normalized pattern as the load curve. Although this proportionality assumption aligns with typical Time-of-Use tariff structures, actual price signals—especially in markets with high renewable penetration—may deviate considerably from load-driven profiles. Future studies should explore the influence of real hourly wholesale market prices or stochastic price forecasting models to evaluate the sensitivity of EV charging and DR performance to diverse tariff conditions.

Third, the current model focuses primarily on economic dispatch, load shifting, and network-level energy losses, without conducting a detailed evaluation of voltage profiles or V2G operational strategies. While voltage constraints are included in the optimization, the study does not analyze spatial voltage behavior or quantify voltage improvement indices across the network. Similarly, V2G discharging is only modeled as an optional flexibility mechanism, and its operational constraints—such as inverter limits, degradation costs, or grid support requirements—are not explicitly captured. Extending the framework to incorporate full V2G operational modeling would enable a deeper understanding of EVs as potential distributed energy resources.

Finally, the analysis is limited to moderate EV penetration conditions. The rapid electrification of transportation may lead to significantly higher adoption levels, which could introduce non-linear grid impacts, greater congestion risks, and more pronounced voltage deviations. Future work should examine extreme penetration scenarios, including neighborhood-level clustering effects, to better understand scalability and resilience under more demanding operating conditions.

5. CONCLUSION

In this study, the impact of EV management — as both controllable loads and energy storage systems — on modifying consumer load profiles was investigated. First, the operation of distribution networks, electric vehicles, distributed generation sources, and EV-DR programs over a 24-hour period were examined from an energy-pricing perspective. The primary objective was to analyze the integration of EV loads into the distribution network and to assess how electricity prices influence EV charging behavior, with the aim of optimizing energy utilization and improving system performance. In addition to EVs, the potential integration of renewable energy sources such as photovoltaic generation was also considered. A DR strategy was implemented in a distribution network with distributed generation and time-varying electricity prices to regulate EV charging throughout the day. The proposed approach sought to minimize operational costs, reduce energy losses, and mitigate voltage drops by accounting for network loading conditions in the presence of EVs. The results showed that DR programs effectively reduced energy losses in the 33-bus network, whereas the inclusion of EVs increased total network losses. Overall, the findings demonstrate that the proposed method can successfully manage EV loads and reduce peak-hour demand, even when uncontrollable renewable sources are present. Furthermore, optimized charging and discharging schedules enhanced network management, contributing to a more stable and efficient power distribution system. However, several limitations should be acknowledged: EV behavior was modeled deterministically, PV generation was represented without detailed irradiance data, and electricity prices were assumed to be fixed. Future work will address these issues by incorporating stochastic EV behavior, dynamic pricing, multi-objective optimization, and additional performance metrics such as voltage stability. These enhancements will enable a more comprehensive and realistic assessment of system performance under uncertainty.

ACKNOWLEDGEMENT

The authors acknowledge the use of artificial intelligence tools (e.g., ChatGPT by OpenAI) for language editing and clarity improvement during the preparation of this manuscript. The authors are fully responsible for the scientific content, analysis, and conclusions.

REFERENCES

[1] I. Ullah, J. Zheng, A. Jamal, M. Zahid, M. Almoshageh, and M. Safdar, "Electric vehicles charging infrastructure planning: A review," *Int. J. Green Energy*, vol. 21, no. 7, pp. 1710–1728, 2024.

[2] F. Al Sharari, O. Yemelyanov, Y. Dziurakh, O. Sokil, and O. Danylovych, "The energy-saving projects' impact on the level of an enterprise's financial stability," *Econ. Ann.-XXI*, vol. 195, no. 1–2, pp. 36–49, 2022.

[3] A. Z. Nazori, G. Brotosaputro, S. Solichin, U. Budiyanto, and D. Mahdiana, "Design and implementation of fuzzy intelligent controller to manage energy resources in a greenhouse system," *Procedia Environ. Sci., Eng. Manag.*, vol. 11, no. 1, pp. 19–25, 2024.

[4] S. M. Mortezaie, "Analysis and design of a soft-switching interleaved boost converter using auxiliary resonant circuit for electric vehicle applications," *Procedia Environ. Sci., Eng. Manag.*, vol. 12, no. 1, pp. 47–54, 2025.

[5] S. Sagaria, M. van der Kam, and T. Boström, "Vehicle-to-grid impact on battery degradation and estimation of V2G economic compensation," *Appl. Energy*, vol. 377, p. 124546, 2025.

[6] B. Pang, H. Zhu, Y. Tong, and Z. Dong, "Optimal design and control of battery–ultracapacitor hybrid energy storage system for BEV operating at extreme temperatures," *J. Energy Storage*, vol. 101, p. 113963, 2024.

[7] Z. Ma, Y. Luan, F. Zhang, S. Xie, and S. Coskun, "A data-driven energy management strategy for plug-in hybrid electric buses considering vehicle mass uncertainty," *J. Energy Storage*, vol. 77, p. 109963, 2024.

[8] A. Q. Al-Shetwi, I. E. Atawi, M. A. El-Hameed, and A. Abuelrub, "Digital twin technology for renewable energy, smart grids, energy storage and vehicle-to-grid integration," *IET Smart Grid*, vol. 8, no. 1, p. e70026, 2025.

[9] S. Dong and S. Guo, "Advancements, challenges, and future trends of vehicle-to-grid technologies: A review," *Energy Technol.*, vol. 13, no. 11, p. 2500481, 2025.

[10] H. Singh, A. Ambikapathy, K. Logavani, G. A. Prasad, and S. Thangavel, "Plug-in hybrid electric vehicles (PHEVs)," in *Electric Vehicles: Modern Technologies and Trends*, pp. 53–72, 2021.

[11] A. Tariq, S. A. A. Kazmi, G. Ali, and A. H. U. Bhatti, "Multivariate stochastic modeling of plug-in electric vehicles charging profile and grid impact analysis," *Sustain. Energy Grids Netw.*, vol. 36, p. 101155, 2023.

[12] A.-M. Hariri, M. A. Hejazi, and H. Hashemi-Dezaki, "Investigation of impacts of plug-in hybrid electric vehicles' stochastic characteristics modeling on smart grid reliability under different charging scenarios," *J. Clean. Prod.*, vol. 287, p. 125500, 2021.

[13] D. Sahu, P. Sinha, S. Prakash, T. Yang, R. S. Rathore, and L. Wang, "A multi-objective optimization framework for smart parking using digital twin pareto front MDP and PSO for smart cities," *Sci. Rep.*, vol. 15, no. 1, p. 7783, 2025.

[14] L. Ning, "Probabilistic modeling and optimization of microgrids with ev parking lots and dispersed generation," *Comput. Electr. Eng.*, vol. 120, p. 109714, 2024.

[15] Z. M. Zenhom, S. H. A. Aleem, A. F. Zobaa, and T. A. Boghdady, "A comprehensive review of renewables and electric vehicles hosting capacity in active distribution networks," *IEEE Access*, 2024.

[16] E. Bicamumakuba, M. Reza, H. Jin, H. Samsuzzaman, K. Lee, and S. Chung, "Multi-sensor monitoring, intelligent control, and data processing for smart greenhouse environment management," *Sensors*, vol. 25, no. 19, p. 6134, 2025.

[17] P. K. Dubey, B. Singh, V. Kumar, and D. Singh, "A novel approach for comparative analysis of distributed generations and electric vehicles in distribution systems," *Electr. Eng.*, vol. 106, no. 3, pp. 2371–2390, 2024.

[18] E. R. Ghadikolaei, A. Ghafouri, and M. Sedighi, "Probabilistic energy management of dgs and electric vehicle parking lots in a smart grid considering demand response," *Int. J. Energy Res.*, p. 5543500, 2024.

[19] R. Nuvvula, E. Devaraj, and K. T. Srinivasa, "A comprehensive assessment of large-scale battery integrated hybrid renewable energy system to improve sustainability of a smart city," *Energy Sources A*, vol. 47, no. 1, pp. 6195–6215, 2025.

[20] D. Zheng and B. Zheng, "Optimization of electric vehicle charging facility layout considering the enhancement of renewable energy consumption capacity and improvement of PSO algorithm," *Energy Inform.*, vol. 8, no. 1, pp. 1–18, 2025.

[21] M. Tan, Z. Zhang, Y. Ren, I. Richard, and Y. Zhang, "Multi-agent system for electric vehicle charging scheduling in parking lots," *Complex Syst. Model. Simul.*, vol. 3, no. 2, pp. 129–142, 2023.

[22] M. R. Pourhassan, M. R. K. Roshandeh, P. Ghasemi, and M. S. S. Bathaee, "A multi-echelon location–routing–inventory model for a supply chain network using NSGA-II and multi-objective whale optimization algorithm," *Int. J. Supply Oper. Manag.*, vol. 12, no. 1, pp. 81–104, 2025.

[23] A. Mohsenzadeh, S. Pazouki, S. Ardalan, and M.-R. Haghifam, "Optimal placing and sizing of parking lots including different levels of charging stations in electric distribution networks," *Int. J. Ambient Energy*, vol. 39, no. 7, pp. 743–750, 2018.

[24] H. Asghari Rad, M. Jafari-Nokandi, and S. M. Hosseini, "Optimal allocation of plug-in electric vehicle parking lots for maximum serviceability and profit in coupled distribution and transportation networks," *Sci. Iran.*, vol. 31, no. 14, pp. 1178–1196, 2024.

[25] H. I. Shaheen, G. I. Rashed, B. Yang, and J. Yang, "Optimal electric vehicle charging and discharging scheduling using metaheuristic algorithms: V2G approach for cost reduction and grid support," *J. Energy Storage*, vol. 90, p. 111816, 2024.

[26] Y. G. Jahed, S. Y. M. Mousavi, and S. Golestan, "Optimal sizing and siting of distributed generation systems incorporating reactive power tariffs via water flow optimization," *Electr. Power Syst. Res.*, vol. 231, p. 110278, 2024.

[27] Y. Mao, Z. Cai, X. Jiao, and D. Long, "Multi-timescale optimization scheduling of integrated energy systems oriented towards generalized energy storage services," *Sci. Rep.*, vol. 15, no. 1, p. 8549, 2025.